Molecular models of lipopeptide detergents: large coiled-coils with hydrocarbon interiors

Evan Kelly[1], Gilbert G. Privé[2], D. Peter Tieleman[1]*

1. Department of Biological Sciences, Structural Biology Research Group, University of Calgary. 2500 University Dr. NW, Calgary, Alberta, Canada T2N1N4. 2.Department of Medical Biophysics and Department of Biochemistry, University of Toronto; Ontario Cancer Institute.

Methods

   General Details. Nine simulations of octamer micelles were performed. Both parallel (N-termini all at one end) and anti-parallel (N-termini alternating with C-termini at each end) helix orientations were simulated from both simulated annealing and idealized starting points. SAMD was used to find 7 starting structures in an attempt to begin solvated MD simulations at a near equilibrated state. The primary focus was on C_{12} acyl chains, with one C_{16} simulation and a C_{20} simulation also included as a control. (See Table S1 for summary of simulations performed). We will adopt the notation of Pn(X) for parallel oriented simulations and similarly An(X) for anti-parallel where n refers to the acyl chain length and X=I, II, III, IDEAL refers to the starting structure used, Roman numerals used for a starting structure produced by simulated annealing to indicate rank and IDEAL for the idealized starting structures, within a set of identical simulations. Because the structural difference between parallel and anti-parallel octameric micelles with C_{12} chains was minimal in the MD simulations, as well as the structural difference between SA/MD models of parallel and anti-parallel C_{16} and C_{20} octamers, we did not do detailed simulations of parallel C_{16} and C_{20} models. Several control simulations of hexameric and decameric micelles are labeled Nx_A/Pn where x is 6 for hexamers and 10 for decamers, A/P stands for anti-parallel or parallel, and n is the acyl chain length.

   Idealized Starting Structures. An idealized LPD monomer was created by attaching two acyl chains in a full *trans* configuration to the ornithine residues of an ideal right handed α-helix in an orientation parallel to the axis of the helix. Eight exact copies of this ideal LPD were placed in a micelle configuration in both parallel and anti-parallel orientations with helical crossing angles of approximately zero and an approximate coiled coil radius of 1.0 nm.

SAMD Structures. A modified procedure of that used by Nilges and Brünger[1, 2] was used in the Crystallography and NMR System[3, 4]. An ideal octamer comprised of solely C_α atoms was created with a helical crossing angle of zero. All other atoms were placed with identical coordinates to that of their residue's C_α atom. The acyl chain carbon atoms, with the exception of the two closest to the bond with the ornithine residue, were instead placed on the central micellar axis with a shift along that axis of 0.5 nm towards the end of their residue. A first stage of molecular dynamics in vacuum, to allow the structure to "grow" out, was performed 100 times to create 100 different structures. The coordinates of the C_α atoms were kept frozen during this growing stage. A harmonic square well restraint was used at this stage to keep the acyl chains inside the micelle by applying a severe penalty if the centre of mass of the two terminal acyl carbons moved farther than 0.75 nm from the centre of the micelle, where arbitrary micellar radii of 0.8 nm, 1.3 nm and 1.4 nm were used when creating the initial C_α octamer for the 12, 16 and 20 carbon length acyl chain micelles, respectively. The C_α atoms were unfrozen and a second stage of dynamics in vacuum was performed to produce 5 structures from each of the 100 produced from the first stage. Each LPD monomer was restrained to each of its adjacent monomers and its diametrically opposed monomer by weak harmonic square well potentials. The harmonic square well acyl restraints from the previous dynamics stage were kept but the penalty distance widened to 1.25 nm. In addition, standard i to i+4 restraints were used to keep each α helix in a reasonable helical structure by applying a weak penalty if hydrogen bond (O-H) lengths exceeded 0.3 nm. The resulting 500 structures for each type of simulation (A12, P12, A16, A20) were ranked by the criteria of final potential energy less the final restraint energy with lowest values ranked highest. The same procedure was used to model hexamers and decamers, with initial C_α micelle geometries and restraints modified appropriately to compensate for the differing aggregation numbers. The goal was to keep the inner micelle volumes and the inter-helix distances appropriate and consistent with the octamer simulations. Initial micelle radii were 0.8 nm and 1.0 nm for the 12 and 16 carbon length hexamers, and 1.0 nm and 1.5 nm for the 12 and 16 carbon length decamers, respectively.

Aqueous MD Simulations. The highest three ranked A12 structures, highest two P12 structures, highest single A16 and highest single A20 were chosen, giving rise to the simulations A12(I), A12(II), A12(III), P12(I), P12(II), A16(I) and A20(I), respectively. The two idealized

starting structures were called A12(IDEAL) and P12(IDEAL). In addition, the highest ranked models of hexameric and decameric parallel and antiparallel bundles with C12 and C16 chains (see table S1) were simulated. Simulations were performed with GROMACS 3.1.3 or on a different linux cluster with the updated and regression-tested GROMACS 3.2.1[5, 6] (the hexameric and decameric models, C0, and P12(II)). All simulations used the GROMOS96 45a3 force field[7]. All simulations used periodic boundary conditions, Lennard-Jones cutoffs of 1.4 nm, short-range electrostatics cutoffs of 0.85 nm, particle mesh Ewald (PME) summation[8] with order 4 spline interpolation and a 0.12 nm grid, and a neighborlist update every 5 steps. Temperature was set to 298K using a Berendsen thermostat (tau = 0.1 ps) coupled separately to solvent, micelle, and ions. Berendsen isotropic pressure coupling (tau = 1.0 ps) was used with a compressibility of 4.5×10^{-5} bar^{-1} and a reference pressure of 1 bar[9]. All LPD starting structures were solvated by SPC water ranging in number between 9921 (for A20) and 12780 (for decamer models). Water molecules were removed if any intermolecular distance from a solvent atom to a solute atom exceeded the sum of the two atom's van der Waals radii. To match the experimental conditions of McGregor et al.[10], 37 Na+ ions and 37 Cl- ions were added to each simulation, except for A20 in which 36 of each ion were added. In particular, 10222 water molecules were used in both A12(I) and P12(II), which therefore have the exact same composition, to make it possible to compare potential energies. The control simulation of the hexamers and decamers have the same composition per peptide (table S1). Simulations were done in a cubic box with sides of ca. 6.4 nm, 7.0 nm, 7.6 nm for hexamers, octamers and decamers, respectively. The total solvated molecular dynamics simulation time was 10ns for each simulation with a time step of 2 fs.

Analysis. Snapshots were rendered using PyMol[11]. RMSDs were calculated at intervals of 1ps for the backbone atoms after fitting on the backbone atoms. Secondary structure was calculated using DSSP[12] at intervals of 5 ps for each entire simulation. For both A12(I) and P12(II) simulations, potential energy standard deviations and statistical block averaged error estimates using the method of Hess[13] were performed over the final 5ns. This method used autocorrelation functions to estimate the number of independent points in a time series. The A12(I) simulation has an average potential energy of -4.84077 105 kJ/mol with a standard deviation of 491 kJ/mol and standard error of 10 kJ/mol, while P12(II) has an average energy of -4.83751 105 kJ/mol, a standard deviation of 484 kJ/mol and a standard error of 9 kJ/mol.

Although the energy difference in the average is less than the standard deviation, the estimated error in the average is much smaller than the average difference and the difference should therefore be considered significant. It remains, however, possible that slower correlations are present due to e.g. bundle dynamics or slow equilibration of salt. This type of correlations would give a systematic error that we expect may be significantly larger than the statistical error, but it is not possible to estimate this error accurately.

Radii of gyration were calculated at intervals of 1ps via:

$$R_g = \sqrt{\frac{\sum\limits_{i=\text{atom index}} m_i r_i^2}{\sum\limits_{i=\text{atom index}} m_i}}$$

where m_i is the mass of each atom, and r is the distance from the centre of mass of the micelle. The radii of gyration procedure was modified to approximate the hydrodynamic radius by the inclusion of a solvent shell in the atoms summed over. Solvent molecules and ions were included in the solvent shell if a solvent atom or an ion was within a cutoff distance of a solute atom. Cutoff distances were modified from the shell cut-off radii used by Brunne[14] by adding approximate molecular or ionic diameters (0.3 nm for water molecules and Na^+ ions and 0.2 nm for smaller Cl^- anions) to Brunne's values. This was intended to give generous cutoff values to ensure that at least a full solvent monolayer was included without a full second layer being added. Hydrophobic and hydrophilic solvent accessible surface areas (SASA) were calculated using the algorithm of Eisenhaber et al.[15] using the default 0.14nm probe radius and are presented as a fraction of hydrophobic area to total area. Dihedral angle trans fractions were calculated for the dihedral angles formed over all acyl chain carbon atoms using the definition of trans as a dihedral angle, ϕ, ranging between 120° and 240° where ϕ is defined to be zero at the cis conformation. Average dihedral transition times were also calculated for the acyl chains. The same dihedral calculations were performed on 512 molecules of liquid phase decane and dodecane in equilibrated boxes over 1 ns of simulation performed under identical simulation details as the solvated micelle simulations. An implementation of the TWISTER algorithm[16] was used to calculate Crick coiled coil heptad repeat assignments, α-helical radii, coiled coil radii and helical crossing angles over the final 5ns of each simulation at intervals of 5ps.

Tables

Table S1. Summary of the simulations. All simulations are 10 ns, with the same simulation conditions unless indicated.

Simulation	Starting structure	System
A20	Top-ranked SA/MD model for LPD micelle with anti-parallel helix orientation, with C20 acyl chains	8 LPD20, 9921 water, 36 Na$^+$, 36 Cl$^-$
A16	Top-ranked SA/MD model for LPD micelle with anti-parallel helix orientation, with C16 acyl chains	8 LPD16, 10050 water, 37 Na$^+$, 37 Cl$^-$
A12(I)	Top-ranked SA/MD model for LPD micelle with anti-parallel helix orientation, with C12 acyl chains	8 LPD12, 10222 water, 37 Na$^+$, 37 Cl$^-$
A12(II)	Second-ranked SA/MD model for micelle with anti-parallel helix orientation, with C12 acyl chains	8 LPD12, 10241 water, 37 Na$^+$, 37 Cl$^-$
A12(III)	Third-ranked SA/MD model for micelle with anti-parallel helix orientation, with C12 acyl chains	8 LPD12, 10221 water, 37 Na$^+$, 37 Cl$^-$
A12(IDEAL)	Model for LPD micelle with anti-parallel helices, initially in ideal helix geometry, with C12 acyl chains	8 LPD12, 10300 water, 37 Na$^+$, 37 Cl$^-$
P12(I)	Top-ranked SA/MD model for LPD micelle with all helices parallel, with C12 acyl chains	8 LPD12, 10214 water, 37 Na$^+$, 37 Cl$^-$
P12(II)	Second-ranked SA/MD model for LPD micelle with all helices parallel, with C12 acyl chains	8 LPD12, 10222 water, 37 Na$^+$, 37 Cl$^-$
P12(IDEAL)	Model for LPD micelle with parallel helices, initially in ideal helix geometry, with C12 acyl chains.	8 LPD12, 10209 water, 37 Na$^+$, 37 Cl$^-$
N6_A12, N6_P12	Top-ranked SA/MD models for hexameric LPD micelle with anti-parallel (N6_A12) or parallel (N6_P12) helices with C12 acyl chains.	6 LPD12, 7668 water, 28 Na$^+$, 28 Cl$^-$
N6_A16, N6_P16	Top-ranked SA/MD models for hexameric LPD micelle with anti-parallel (N6_A16) or parallel (N6_P16) helices with C16 acyl chains.	6 LPD16, 7668 water, 28 Na$^+$, 28 Cl$^-$
N10_A12, N10_P12	Top-ranked SA/MD models for decameric LPD micelle with anti-parallel (N10_A12) or parallel (N10_P12) helices with C12 acyl chains.	10 LPD12, 12780 water, 46 Na$^+$, 46 Cl$^-$
N10_A16, N10_P16	Top-ranked SA/MD models for decameric LPD micelle with anti-parallel (N10_A16) or parallel (N10_P16) helices with C16 acyl chains.	10 LPD16, 12780 water, 46 Na$^+$, 46 Cl$^-$
C0	Started from final structure of P12(I) with the acyl chains deleted and the ornithine residues restored (30 nanoseconds).	8 LPD12, 10411 water, 37 Na$^+$, 53 Cl$^-$

Table S2. Comparison of Coiled-coil structures.

	GCN4	GCN4	GCN4	COMP	Trp14	P12	A12	A16	A20
number of helices	dimer	trimer	tetramer	pentamer	pentamer	octamer	octamer	octamer	octamer
α-helix									
radius (R1) (A)	2.28	2.24	2.26	2.2	2.06	2.31	2.4	2.31	2.3
rise/residue (d) (A)	1.51	1.53	1.52	1.52	1.49	1.52	1.51	1.51	1.5
residues/turn	3.62	3.6	3.59	3.58	3.6	3.64	3.68	3.65	3.6
crossing angle (degrees)	23.4	23.2	18.3	18.5	14	4.5	8.7	10	6.7
interhelical distance (A)	9.8	11.5	10.6	10.2	11.2	9.1	9.2	9.5	9.7
coiled-coil superhelix									
radius (A)	4.9	6.7	7.6	8.6	9.7	11.2	11.6	12.3	12.7
pitch (A)	148	175	205	204	277	840*	283	372	500
residues/turn	100	118	139	140	190	560*	194	256	345

Experimentally determined structures are shaded. The values reported are from the original papers. The GCN4 structures are from Harbury et al.[17], COMP is from Malashkevich et al.[18], Trp14 is from Liu et al.[19]. P12, A12, A16 and A20 are from this work, calculated from the final structures after 10 ns of simulation.

* Because the helices are nearly parallel to the superhelix axis, these values are poorly determined.
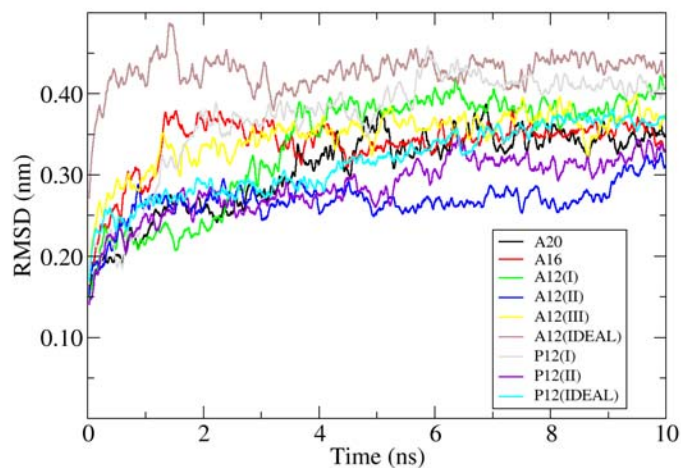
Figures

Figure S1. Root mean square deviation from the starting structure as a function of time for 9 simulations. Data have been averaged over 25 ps windows.
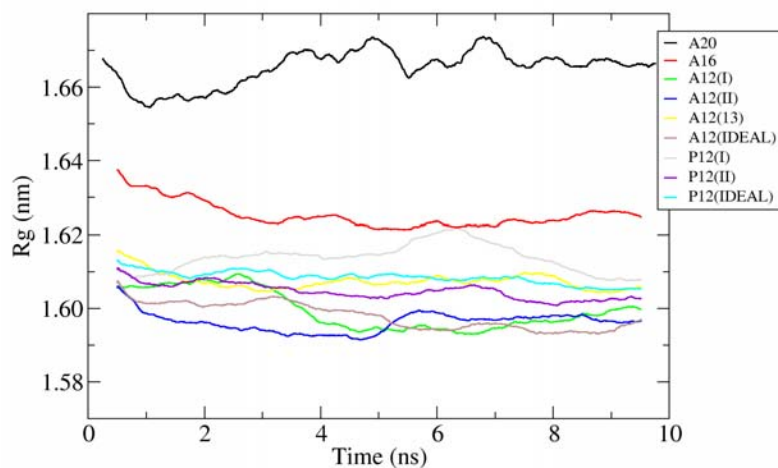

Figure S2. The radius of gyration of the micelle models as a function of time. Data have been averaged over 250 ps windows.
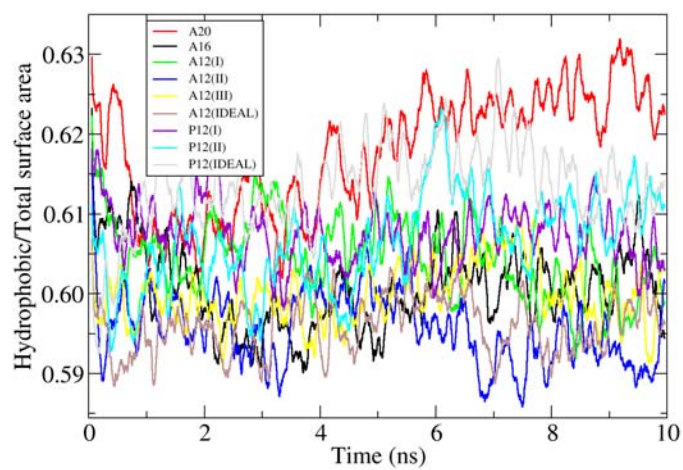
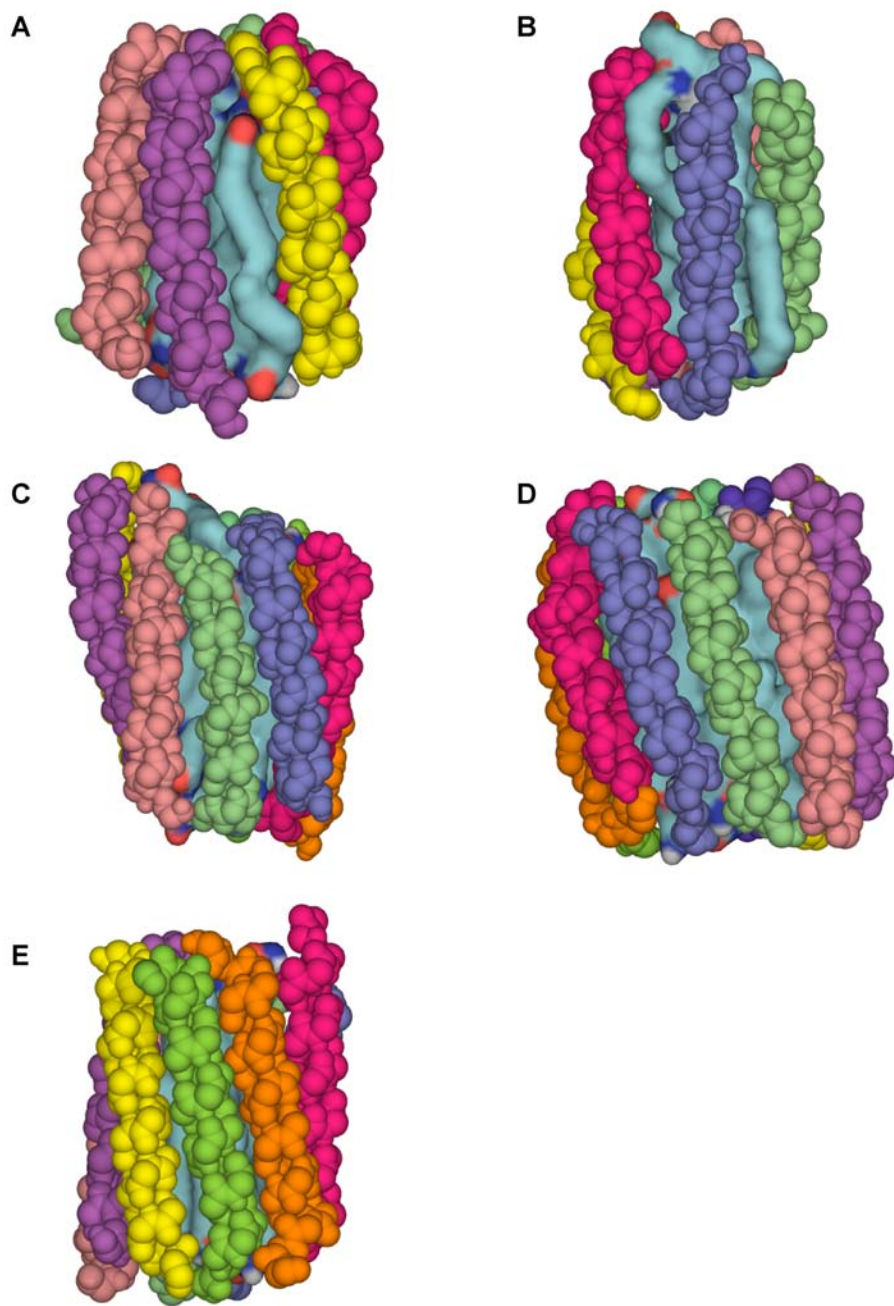**Figure S3.** The ratio of hydrophobic and total surface area as a function of time, averaged over 25 ps windows.

Figure S4. Snapshots after 10 ns of four of the control simulations and a stable octamer. **A**. The hexamer N6-PC12. **B**. The hexamer N6-AC16. **C**. The decamer N10-AC12. **D**. The decamer N10-AC16. **E**. The stable octamer A12(II). The space filling models are for main-chain atoms of the peptides only. Side chains are deleted. The alkyl chains are in surface representation with blue carbons.
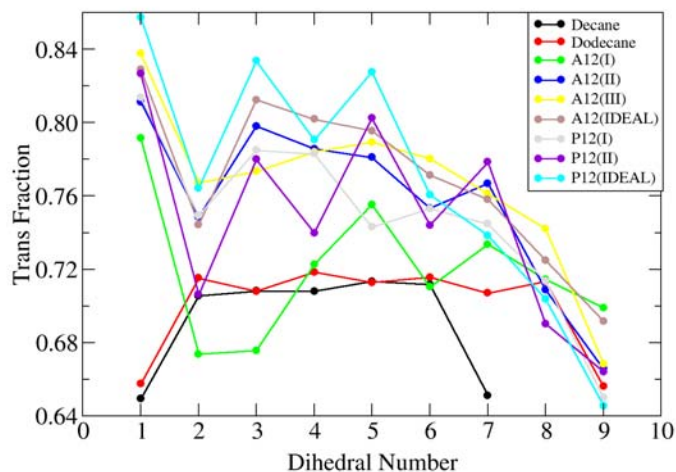
Figure S5. The average fraction of acyl chain dihedrals in the *trans* conformation. For comparison, the results from liquid decane and dodecane at the same temperature are also shown.
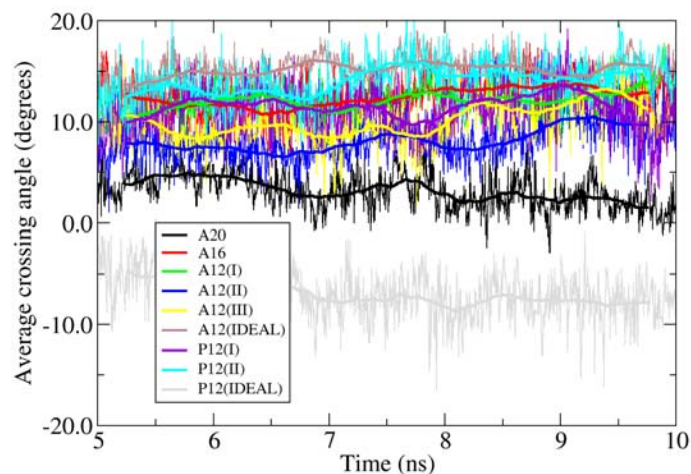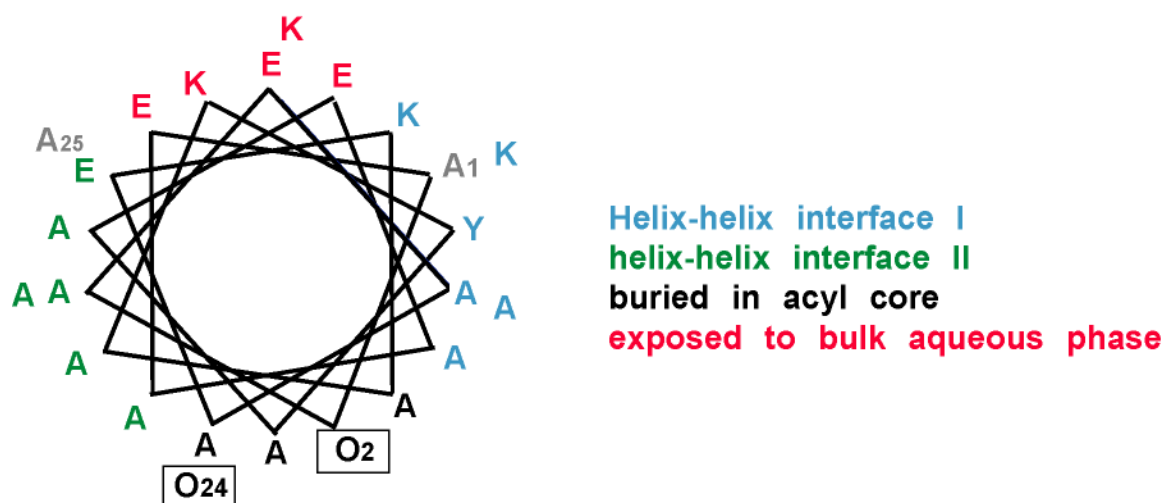

Figure S6. The helical crossing angle over the last 5 ns as defined by TWISTER (thin lines), together with the same value averaged over 250 ps windows (thick lines).

Figure S7. Assignment of the peptide residues to four different environments. The helical wheel is based on a helix twist angle of 100°.

References

1. Nilges, M.; Brunger, A. T., Automated modeling of coiled coils: application to the GCN4 dimerization region. *Protein Eng* **1991,** 4, (6), 649-59.
2. Nilges, M.; Brunger, A. T., Successful prediction of the coiled coil geometry of the GCN4 leucine zipper domain by simulated annealing: comparison to the X-ray structure. *Proteins* **1993,** 15, (2), 133-46.
3. Ash, W. L.; Stockner, T.; MacCallum, J. L.; Tieleman, D. P., Computer modeling of polyleucine-based coiled coil dimers in a realistic membrane environment: insight into helix-helix interactions in membrane proteins. *Biochemistry* **2004,** 43, (28), 9050-60.
4. Brunger, A. T.; Adams, P. D.; Clore, G. M.; DeLano, W. L.; Gros, P.; Grosse-Kunstleve, R. W.; Jiang, J. S.; Kuszewski, J.; Nilges, M.; Pannu, N. S.; Read, R. J.; Rice, L. M.; Simonson, T.; Warren, G. L., Crystallography & NMR system: A new software suite for macromolecular structure determination. *Acta Crystallogr D Biol Crystallogr* **1998,** 54, (Pt 5), 905-21.
5. Lindahl, E.; Hess, B.; van der Spoel, D., GROMACS 3.0: a package for molecular simulation and trajectory analysis. *Journal of Molecular Modeling* **2001,** 7, (8), 306-317.
6. Berendsen, H. J. C.; van der Spoel, D.; van Drunen, R., GROMACS: A message-passing parallel molecular dynamics implementation. *Comp. Phys. Comm.* **1995,** 95, 43-56.
7. Schuler, L. D.; Daura, X.; Van Gunsteren, W. F., An Improved GROMOS96 Force Field for Aliphatic Hydrocarbons in the Condensed Phase. *Journal of Computational Chemistry* **2001,** 22, (11), 1205-1218.

8.   Essmann, U.; Perera, L.; Berkowitz, M. L.; Darden, T.; Lee, H.; Pedersen, L. G., A Smooth Particle Mesh Ewald Method. *Journal of Chemical Physics* **1995,** 103, (19), 8577-8593.

9.   Berendsen, H. J. C.; Postma, J. P. M.; Vangunsteren, W. F.; Dinola, A.; Haak, J. R., Molecular-Dynamics with Coupling to an External Bath. *Journal of Chemical Physics* **1984,** 81, (8), 3684-3690.

10.   McGregor, C. L.; Chen, L.; Pomroy, N. C.; Hwang, P.; Go, S.; Chakrabartty, A.; Prive, G. G., Lipopeptide detergents designed for the structural study of membrane proteins. *Nat Biotechnol* **2003,** 21, (2), 171-6.

11.   DeLano, W. L. *The PyMOL Molecular Graphics System*, DeLano Scientific: San Carlos, California, 2002.

12.   Kabsch, W.; Sander, C., Dictionary of Protein Secondary Structure - Pattern-Recognition of Hydrogen-Bonded and Geometrical Features. *Biopolymers* **1983,** 22, (12), 2577-2637.

13.   Hess, B., Convergence of sampling in protein simulations. *Phys Rev E Stat Nonlin Soft Matter Phys* **2002,** 65, (3 Pt 1), 031910.

14.   Brunne, R. M.; Liepinsh, E.; Otting, G.; Wuthrich, K.; van Gunsteren, W. F., Hydration of proteins. A comparison of experimental residence times of water molecules solvating the bovine pancreatic trypsin inhibitor with theoretical model calculations. *J Mol Biol* **1993,** 231, (4), 1040-8.

15.   Eisenhaber, F.; Lijnzaad, P.; Argos, P.; Sander, C.; Scharf, M., The Double Cubic Lattice Method - Efficient Approaches to Numerical-Integration of Surface-Area and Volume and to Dot Surface Contouring of Molecular Assemblies. *Journal of Computational Chemistry* **1995,** 16, (3), 273-284.

16.   Strelkov, S. V.; Burkhard, P., Analysis of alpha-helical coiled coils with the program TWISTER reveals a structural mechanism for stutter compensation. *J Struct Biol* **2002,** 137, (1-2), 54-64.

17.   Harbury, P. B.; Kim, P. S.; Alber, T., Crystal structure of an isoleucine-zipper trimer. *Nature* **1994,** 371, (6492), 80-3.

18.   Malashkevich, V. N.; Kammerer, R. A.; Efimov, V. P.; Schulthess, T.; Engel, J., The crystal structure of a five-stranded coiled coil in COMP: a prototype ion channel? *Science* **1996,** 274, (5288), 761-5.

19.   Liu, J.; Yong, W.; Deng, Y.; Kallenbach, N. R.; Lu, M., Atomic structure of a tryptophan-zipper pentamer. *Proc Natl Acad Sci U S A* **2004,** 101, (46), 16156-61.